Volume 9, December 2020 ISSN 2542-2545

The HIMALAYAN PHYSICS

A peer-reviewed Journal of Physics

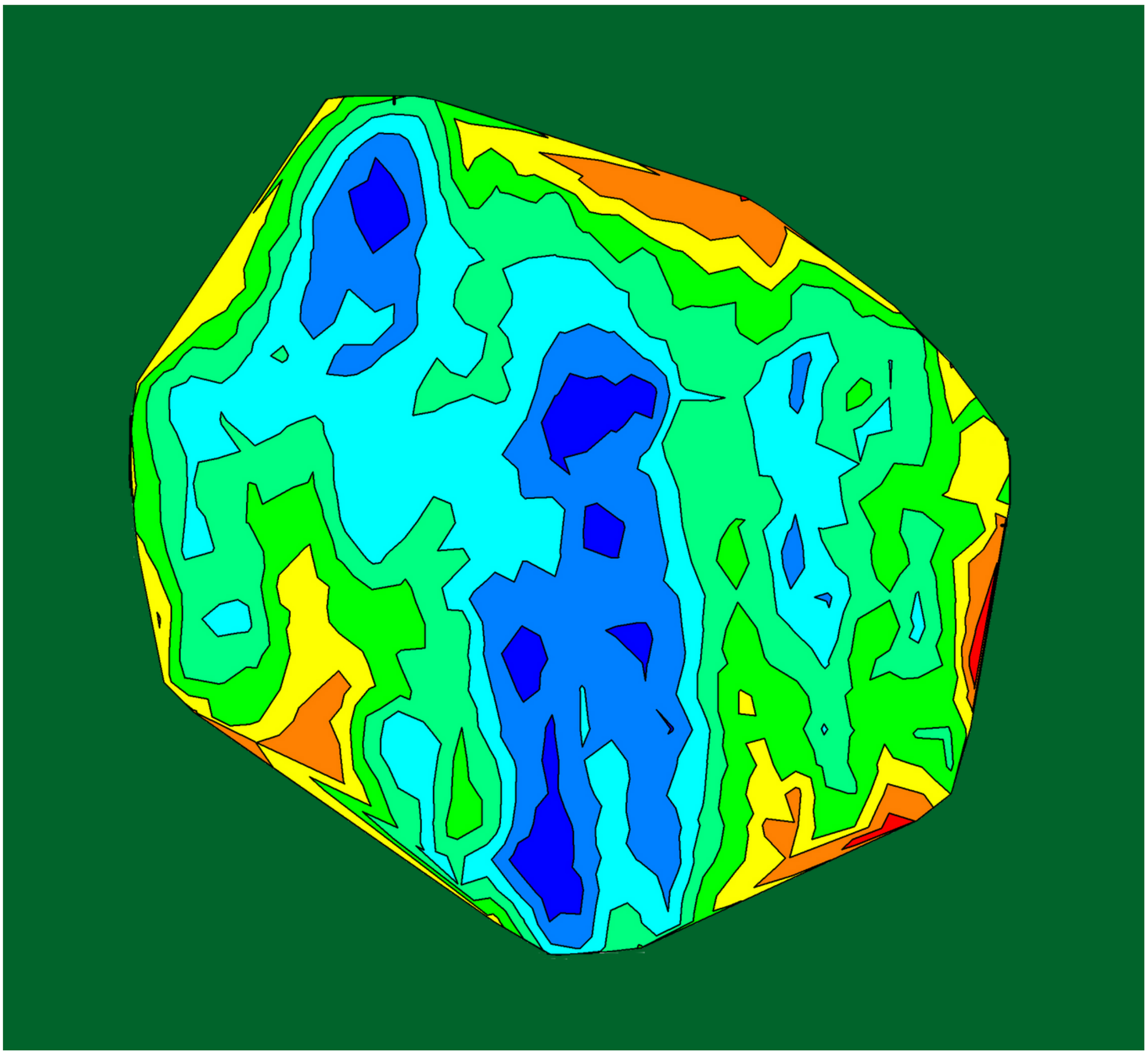

Department of Physics, Prithvi Narayan Campus, Pokhara
Nepal Physical Society, Western Chapter, Pokhara

Publisher

Department of Physics, Prithvinarayan Campus, Pokhara
Nepal Physical Society, Western Chapter, Pokhara

The Himalayan Physics

Volume 9, December 2020

ISSN 2542-2545

The Himalayan Physics (HimPhys) is an open access peer-reviewed journal that publishes quality articles which make innovative contributions in all areas of Physics. HimPhys is published annually by Nepal Physical Society (Western Regional Chapter), and Department of Physics, Prithvi Narayan Campus, Pokhara. The goal of this journal is to bring together researchers and practitioners from academia in Nepal and abroad to focus on advanced techniques and explore new avenues in all areas of physical sciences and establishing new collaborations with physics community in Nepal.

Cover: Contour map of dust mass. © Mijas Tiwari. Printed from article in the current issue, with permission.

Volume 9, December 2020 ISSN 2542-2545

The HIMALAYAN PHYSICS

A peer-reviewed Journal of Physics

Publisher
Department of Physics, Prithvi Narayan Campus, Pokhara
Nepal Physical Society, Western Chapter, Pokhara

Nepal Physical Society

Western Regional Chapter

Pokhara, Nepal

Himalayan Physics Vol-9 (2020)

TABLE OF CONTENTS

****

Him. Phys. **9** 19-29, (2020)

Himalayan Physics

First-principles study of C cites vacancy defects in water adsorbed Graphene

Research Article

Hari Krishna Neupane[1,2], Narayan Prasad Adhikari[2]*

1 Amrit Campus, Institute of Science and Technology Tribhuvan University, Kathmandu, Nepal

2 Central Department of Physics, Institute of Science and Technology Tribhuvan University, Kathmandu, Nepal

Abstract: The electronic and magnetic properties of water adsorbed graphene ($w_{ad}-G$), single carbon (1C) atom vacancy defects in water adsorbed graphene ($1C_{atom\text{-}vacancy}-w_{ad}-G$) and double carbon (2C) atoms vacancy defects in water adsorbed graphene ($2C_{atoms\text{-}vacancy}-w_{ad}-G$) materials are studied by first-principles calculations within the frame work of density functional theory (DFT) using computational tool Quantum ESPRESSO (QE) code. We have calculated the binding energy of $w_{ad}-G$, $1C_{atom\text{-}vacancy}-w_{ad}-G$ and $2C_{atoms\text{-}vacancy}-w_{ad}-G$ materials, and then found that non-defects geometry is more compact than vacancy defects geometries. From band structure calculations, we found that $w_{ad}-G$ is zero band gap semiconductor, but $1C_{atom\text{-}vacancy}-w_{ad}-G$ and $2C_{atoms\text{-}vacancy}-w_{ad}-G$ materials have metallic properties. Hence, zero band gap semiconductor changes to metallic nature due to C sites vacancy defects in its structures. We have investigated the magnetic properties of $w_{ad}-G$ and its C sites vacancy defects materials by using Density of States (DOS) and Partial Density of States (PDOS) calculations. We found that $w_{ad}-G$ is non- magnetic material. 1C atom vacancy defects in graphene surface of $w_{ad}-G$ is induced magnetization by the rebonding of two dangling bonds and acquiring significant magnetic moment ($-0.11\ \mu_B/\text{cell}$) through remaining unsaturated dangling bond. But, 2C atoms vacancy defects in graphene surface of $w_{ad}-G$ induced low value of magnetic moment ($+0.03\ \mu_B/\text{cell}$) than 1C atom vacancy defects in structure, which is due to no dangling bonds present in the structure. Therefore, non-magnetic $w_{ad}-G$ changes to magnetic $1C_{atom\text{-}vacancy}-w_{ad}-G$ and $2C_{atoms\text{-}vacancy}-w_{ad}-G$ materials due to C sites vacancy defects in $w_{ad}-G$ structure. The 2p orbital of carbon atoms has main contribution of magnetic moment in defects structures.

Keywords: • DFT • Vacancy defects • Water adsorbed Graphene • Magnetic moment

1. Introduction

Graphene is a carbon allotrope with a two dimensional (2D) honeycomb lattice. The honeycomb network made by planar and three-folded sp^2 hybrid orbitals acquires planar stability through $\pi-\pi$ orbital interaction and achieves high in-plane stiffness [1]. Dirac cones provided by the linearly crossing π and π^* bands meet as six points in k -space, and is called zero band gap semiconductor. Graphene has various exceptional properties, such as high mechanical strength, chemical stability, massless Dirac fermions behavior, ambipolar effect, unique electronic and magnetic properties [2–5] . It is used for the fabrication of electronic devices, transparent electrodes

* *Corresponding Author: narayan.adhikari@cdp.tu.edu.np*

and spintronics devices [6–8]. So, graphene has opened up exciting opportunities for developing nanoelectronic devices. However, the lack of intrinsic band gap and non-magnetic nature of graphene limits its practical applications in widely expanding field of carbon- based devices. The chemical and physical properties of materials are affected by the structural defects in low dimensional systems. Defects are expected to play key roles in the chemical functionally and electronic transport properties of graphene based materials. The understanding of the mechanical, electrical and magnetic properties of defects in graphene is an important applied physics goal [1, 9]. So, defects in graphene provide an opportunity for the researchers. The vacancies in monolayer structures of graphene have attracted various experimental and theoretical studies [10–16]. Vacancy defects graphene material enhanced the catalytic activities of materials. So, scientists developed vacancy defects in 2D honeycomb structure of graphene, although it has high defects formation energy in comparison with other 2D materials [17, 18]. Both theoretical and experimental research groups have studied the mechanical, electronic and magnetic properties of single carbon atom vacancy defects in graphene. They found that a single carbon atom vacancy defects in graphene is able to induce local magnetic moments due to the three carbon dangling bond atoms surrounding a single vacancy [19–22]. The adsorption of new material in graphene and its vacancy defects materials tunes more desirable properties than pristine graphene only. To our best knowledge, electronic and magnetic properties of carbon atom vacancy defects in water adsorbed graphene structure have not been reported. Therefore, in present work, we have investigated the electronic and magnetic properties of single and double carbon atom vacancy defects in water adsorbed graphene structure through first-principles calculations within spin polarized density functional theory (DFT) method, using computational tool Quantum ESPRESSO package.

The rest part of the paper is organized as follows. In section 2, we discuss details of computational methods. The results and their interpretations are given in section 3. We closed the paper with main conclusions and outlook of the present work in section 4.

2. Computational Details

We have performed spin polarized Density Functional Theory (DFT) calculations [23] , within the generalized gradient approximation (GGA) using computational tool Quantum ESPRESSO package [24, 25] and structure analysis tool XCrySDen. The exchange-correlation potential is approximated with Perdew-Burke-Ernzerhof (PBE) functional [25]. The Rappe-Rabe-Kaxiraas-Joannopoulos (RRJK) model of ultra-soft pseudo-potential is used to incorporate the activity of valence electrons in all the calculations. A vacancy defects honeycomb structure is represented by (4×4) the super cell structure of monolayer graphene sheet. The brillouin zone was sampled by $(6 \times 6 \times 1)$ k-points in the Monkhorst-Pack (MP) scheme [26], where the convergence in energy as a function of the number of k-points was tested. A plane wave basis set with energy cut- off value of (35Ry) and charge density cut-off value (350Ry) was used for the expansion of ground state electronic wave function. Atomic positions were optimized by using the Broyden-Fletcher-Goldfarb-Shanno (BFGS) scheme [27], until the total energy changes

between two consecutive self consistent field (SCF) steps is less than 10^{-4}Ry and each component of force acting is less than 10^{-3}Ry/Bohrs. Moreover, we used Marzarri-Vanderbilt (MV) [28] method of 'smearing' having width of 0.001 Ry. Also, we have chosen 'david' diagonalization method with 'plain' mixing mode and mixing factor of 0.6 for self consistency. We used spin polarized calculations for magnetic properties of the systems. The meshes of $(6 \times 6 \times 1)$ k-points is used for electronic band structure and $(12 \times 12 \times 1)$ k-points is used for DOS & PDOS calculations, where 100 k-points are used along the high symmetric points connecting the reciprocal space for bands structure calculations. In the present work, we have prepared water adsorbed in (4×4) super cell structure of graphene and 1C & 2C atoms vacancy defects in water adsorbed graphene structure as shown in fig. $1(a-e)$. These 1C and 2C atoms vacancy defects in water adsorbed graphene structures are constructed by removing centre 1C atom and 2C (left 1C & centre 1C) atoms in (4×4) super cell structure of graphene. After that, these structures are optimized and relaxed by BFGS method, which are used for further calculations as shown in fig. 1 .

3. Results and Discussion

This section mainly focused on the results and interpretations of geometrical structures band structure calculations, Density of States (DOS), and Partial Density of States (PDOS) calculations, of 1C & 2C atoms vacancy defects in graphene surface of water adsorbed graphene by first-principles calculations including spin polarized DFT method using computational tool Quantum ESPRESSO code.

Electronic Properties

The (4×4) super cell structure of Graphene is made by extending optimized primitive unit cell along x and y directions. The distance between two nearest carbon atoms in graphene is 1.42 [29] . This value agrees with experimentally reported value 1.42 [28]. Here, we have also done the relax calculation of (4×4) super cell structure of graphene until the convergence is achieved, then we performed self consistent field (SCF) calculations of super cell structure to get total energy, binding energy and binding energy per atom. The binding energy and binding energy per atom of super cell structure are calculated by using following formalism;

$$E_b = NE_c - E_g \tag{1}$$

Where, E_g is the ground state energy of pure graphene sheet, E_c is ground state energy of isolated carbon atom and N is the number of carbon atom in a graphene super cell. Similarly, the binding energy per carbon atom is calculated by the relation;

$$\mathrm{E_{b/C-atom}} = \left(\mathrm{NE_c} - \mathrm{E_g}\right)/\mathrm{N} \tag{2}$$

The calculated values of total ground state energy, energy of isolated carbon atom, binding energy, and binding energy per carbon atom for graphene sheet containing $2C$ and 32C atoms (i.e. 32 carbon atoms are presented in

(4×4) super cell structure of graphene) are; −22.80 Ry, −10.98 Ry, 11.44 eV, 5.72 eV/atom, and −397.78 Ry, −11.84 Ry, 255.44 eV, 7.98 eV/atom respectively. The adsorption of water molecule at 2.64 distance above the surface of (4 × 4) super cell structure of graphene as shown in fig. 1(a) does not bring significant changed in the values of pure graphene structure. Also, band structure plot of water adsorbed in graphene ($w_{ad} - G$) as shown in fig. 2(a) is similar with band plot of pure super cell structure of graphene. This is because; the $w_{ad} - G$ structure has no dangling bonds present along the external surface of Graphene which therefore show a reduced chemical activity. Only physisorption interactions can arise when adsorbing water molecule in this structure. This is evidenced by the adsorption energy we calculated for isolated water physisorption on monolayer Graphene (0.12eV) at 2.64 distance of water molecule above the graphene. In the present work, we intended to investigate physical properties of C sites vacancy defects in graphene surface of water adsorbed graphene super cell structure.

Vacancy defects are localized states. They give rise to localized states in the band gap. In our study, we treated the vacancy defects by removing 1C (centre 1C) atom in $w_{ad} - G$ structure ($1C_{\text{atom-vacancy}} - w_{ad} - G$) and 2C (1 left & 1C centre) atoms in $w_{ad} - G$ structure ($2C_{\text{atoms-vacancy}} - w_{ad} - G$) as shown in fig. 1(b − c) and fig. 1(d − e) respectively.

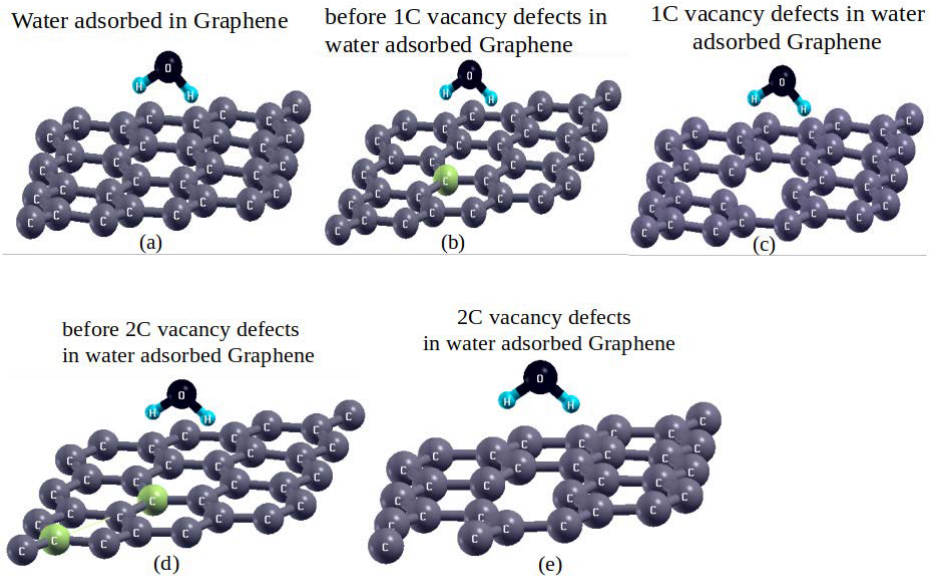

Figure 1. Optimized and relaxed structures of Graphene and C sites vacancy defects in water adsorbed Graphene, where adsorbed water molecule is at 2.64 distance above the surface of Graphene. These structures are constructed by removing 1C & 2C atoms in water adsorbed Graphene material (a) Water adsorbed Graphene structure (b) Before 1C atom vacancy defects in water adsorbed Graphene structure (c) 1C atom vacancy defects in water adsorbed Graphene structure (d) Before 2C atoms vacancy defects in water adsorbed Graphene structure (e) 2C atoms vacancy defects in water adsorbed Graphene structure.

The defects formation energy of single and double carbon atoms vacancy defects in $w_{ad} - G$ structure are 7.6 eV and 7.0 eV respectively, because binding energy of 1C defects is greater than 2C defects in $w_{ad} - G$ structure

as given in table 1. Defects formation energy values of these materials are calculated by using the relation [30].

$$E_f = E_T(defect) + n_C\mu_C - E_T(perfect) \tag{3}$$

Where, E_T (defect) is a total energy of a super cell with the defects, n_C is the numbers of C atoms removed from the perfect super cell to introduce a vacancy, μ_C is chemical potential of C atom, E_T (perfect) is the total energy of the neutral perfect super cell. Defects concentrations of 1C and 2C atoms in structures are 3.125% and 6.25% respectively. For $w_{ad} - G$, if the mesh of vacancy defects in $2D$ hexagonal lattice breaks the specific symmetries of parent pristine $w_{ad} - G$ structure the linearly crossing bands at Fermi level. So, C sites vacancy defects with above mentioned concentrations in $w_{ad} - G$ are seen still have linearly crossing bands, and localized vacancy states corresponding to the flat impurities bands in band gaps as shown in fig. 3 (a) & 4 (a) respectively. Due to symmetry of the super cell having 1C vacancy defects, the linearly crossing bands split and they are raised slightly above the Fermi level. The π and π^* bands around Fermi level mix with the orbitals of vacancy. The states associated with the dangling bond and reconstructed $C - C$ bond of vacancy occurs near the top of valence band and in the conduction band appear as flat bands and charge densities are associated these bands are localized as shown in fig. 3 (a). But, in 2C vacancy defects in $w_{ad} - G$ structure, there is no states associated with dangling bond and reconstructed $C - C$ bond of vacancy occurs around the Fermi energy level as shown in fig. 4 (a). In C sites vacancy defects $w_{ad} - G$ structures, the edges and vacancies are very sensitive locations for molecular adsorption due to the under-coordination of atoms in the edge or around the vacancy. They also play a special role either in determining the geometrical conformation of layered materials and inducing modifications of the electronic properties of the layers itself. Therefore, from the band structures analysis, we found that $1C_{atom\text{-}vacancy} - w_{ad} - G$ and $2C_{atoms\text{-}vacancy} - w_{ad} - G$ materials have metallic nature. We know that the electronic configurations of valence electrons in C, O and H atoms are [He] $2s^2\ 2p^2$, [He] $2s^2\ 2p^4$ and $1s^1$ respectively. Each C atom has single up spin in $2p_x, 2p_y$ and vacant in $2p_z$ sub - orbital, each O atom contains paired spins in $2p_x$ sub - orbital and single unpaired up spin in $2p_y$ and $2p_z$ sub - orbital, and H atom has single unpaired up spin in 1s orbital. Due to the arrangement of unpaired up and down spins states of electrons in the orbitals of atoms in all $w_{ad} - G$, $1C_{atom\text{-}vacancy} - w_{ad} - G$ and $2C_{atoms\text{-}vacancy} - w_{ad} - G$ materials develop different values of Fermi energy. We found that Fermi energy values of these materials are -2.91 eV, -3.29 eV and -3.42 eV respectively. Also, we calculated Fermi energy shift values of $1C_{atom\text{-}vacancy} - w_{ad} - G$ and $2C_{atoms\text{-}vacancy} - w_{ad} - G$ materials are 0.38 eV and 0.51 eV respectively as given in table 1.

Table 1. Fermi energy (E_f), Fermi energy shift (E_s), adsorption energy of water molecule in graphene (E_a), defects formation energy (E_d), binding energy per carbon atom of pure graphene and vacancy defects graphene in $w_{ad}-G$ structures (E_b), total value of magnetic moment (M), and magnetic moment due to total up & down spins of electrons in 2s, 2p orbitals of C & O atoms and 1s orbital of H atoms (μ) in water adsorbed Graphene ($w_{ad}-G$) and C sites vacancy defects in water adsorbed Graphene ($C_{atom\text{-}vacancy}-w_{ad}-G$) materials.

Data of band structures and DOS/PDOS plots of $w_{ad}-G$ & $C_{atom\text{-}vacancy}-w_{ad}-G$	$w_{ad}-G$	$1C_{atom\text{-}vacancy}$ $w_{ad}-G$	$2C_{atom\text{-}vacancy}$ $w_{ad}-G$
E_f(eV)	-2.91	-3.29	-3.42
E_s(eV)	-	0.38	0.51
E_a(eV)	0.12	-	-
E_d(eV)	-	7.60	7.00
E_b(eV)	7.98	7.46	6.82
μ due to 2s of C atoms (μ_B/cell)	0.00	-0.01	0.01
μ due to 2p of C atoms (μ_B/cell)	0.00	-0.10	0.02
μ due to 2s of O atoms (μ_B/cell)	0.00	0.00	0.00
μ due to 2p of O atoms (μ_B/cell)	0.00	0.00	0.00
μ due to 1s of H atoms (μ_B/cell)	0.00	0.00	0.00
Total value of magnetic moment M (μ_B/cell)	0.00	-0.11	+0.03

In addition, we have carried out Density of States (DOS) and Partial Density of States (PDOS) calculations to understand the electronic and magnetic properties of materials more clearly. The DOS and PDOS plots of $w_{ad}-G$, $1C_{atom\text{-}vacancy}-w_{ad}-G$ and $2C_{atom\text{-}vacancy}-w_{ad}-G$ materials are shown in fig. 2(b−c), fig. 3(b−c) and fig. 4(b − c) respectively, where vertical dotted line represents Fermi energy levels of respective structures.

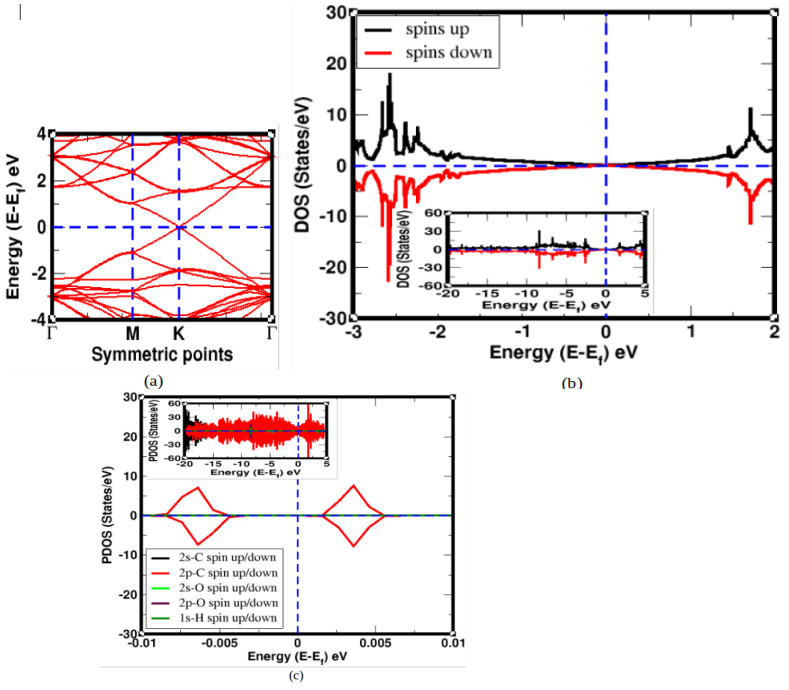

Figure 2. (a) Band structure plot of water adsorbed Graphene (b) Total DOS of up and down spins states of atoms in water adsorbed Graphene (c) PDOS of individual up and down spins states of all atoms in water adsorbed Graphene. In band structure, horizontal dotted line represents Fermi energy level, and in DOS/PDOS plots, vertical dotted line represents Fermi energy level.

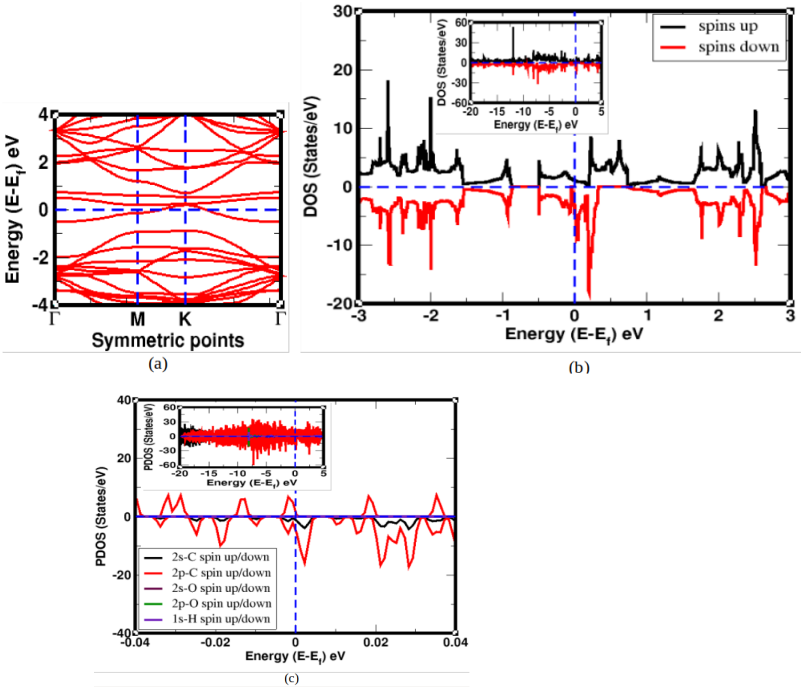

Figure 3. (a) Band structure plot of 1C atom vacancy defects in water adsorbed Graphene (b) Total DOS of up and down spins states of 1C atom vacancy defects in water adsorbed Graphene (c) PDOS of individual up and down spins states of orbitals of 1C atom vacancy defects in water adsorbed Graphene. In band structure, horizontal dotted line represents Fermi energy level, and in DOS/PDOS plots, vertical dotted line represents Fermi energy level.

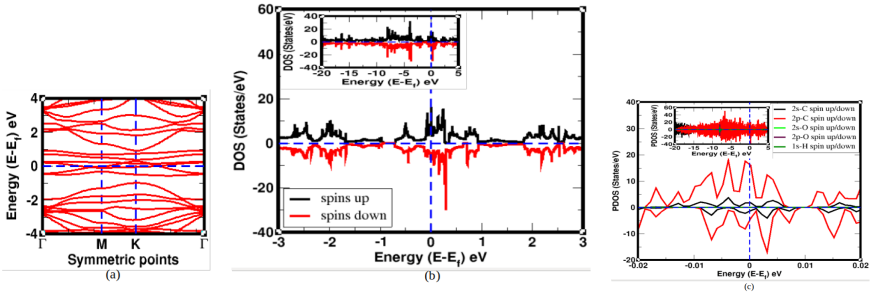

Figure 4. (a) Band structure plot of 2C atoms vacancy defects in water adsorbed Graphene (b) Total DOS of up and down spins states of 2C atoms vacancy defects in water adsorbed Graphene (c) PDOS of individual up and down spins states of orbitals of 2C atoms vacancy defects in water adsorbed Graphene. In band structure, horizontal dotted line represents Fermi energy level, and in DOS/PDOS plots, vertical dotted line represents Fermi energy level.

Magnetic properties

The magnetic and non-magnetic materials are investigated by the analysis of spins distribution in DOS and PDOS plots. The asymmetrically distributed up and down spins states of electrons in DOS and PDOS plots means, materials have magnetic properties, and symmetrically distributed up and down spins states of electrons

in DOS and PDOS plots means, materials carry non-magnetic properties. We observed that up and down spin states of electrons are symmetrically distributed in DOS and PDOS plots of $w_{ad} - G$ material as shown in fig. $2(b - c)$. Net values of magnetic moment are given by up and down spins states of electrons in 2s & 2p orbitals of C & O atoms, and 1s orbital of H atoms in structure is $0.00\mu_B$/cell. Hence, $w_{ad} - G$ is non-magnetic material.

Furthermore, we have analyzed the DOS/PDOS calculations of $1C_{atom\text{-}vacancy} - w_{ad} - G$ and $2C_{atoms\text{-}vacancy} - w_{ad} - G$ materials. The DOS and PDOS of up and down spins states of electrons near the Fermi level are asymmetrically distributed in $1C_{atom\text{-}vacancy} - w_{ad} - G$ as shown in Fig. 3(b−c), because electrons spins degeneracy of the bands are broken and bands split. Hence, $1C_{atom\text{-}vacancy} - w_{ad} - G$ material has magnetic properties. Also, we have calculated the contributions of magnetic moment due to the distribution of spins of electrons in the individual orbital of atoms presented in $1C_{atom\text{-}vacancy} - w_{ad} - G$ material as given in table 1. The magnetic moment developed in material due to up and down spins of electrons in 2s & 2p orbitals of C atoms only which are -0.01 μ_B/cell & -0.10 μ_B/cell respectively. It means, dominant contributions of magnetic moment are given by spins of 2p orbital of C atoms only in the material. The values of magnetic moment are calculated by subtraction between the values of magnetic moment given by total up & down spins states of electrons in the orbitals of atoms present in $1C_{atom\text{-}vacancy} - w_{ad} - G$ material. Hence, from these calculations, we found that total magnetic moment of $1C_{atom\text{-}vacancy} - w_{ad} - G$ has value -0.11 μ_B/cell. Similarly, we have calculated the magnetic moment in $2C_{atoms\text{-}vacancy} - w_{ad} - G$. We know that double vacancy defects in graphene have zero value of magnetic moment because no dangling bonds are formed there. However, in our case, we have obtained small value of magnetic moment which is due to the adsorption of water molecule in double vacancy defects graphene sheet. The DOS/PDOS of up and down spins states of electrons are asymmetrically distributed near the Fermi energy level as shown in fig. 4(b − c). Magnetic moment is given by spins states of electrons in the 2s & 2p orbitals of carbon atoms in structure are 0.01 μ_B/cell & 0.02 μ_B/cell respectively. Hence, total value of magnetic moment of $2C_{atoms\text{-}vacancy} - w_{ad} - G$ material is 0.03 μ_B/cell. The negative value of magnetic moment means, down spins of electrons have dominant role than up spins of electrons, and positive value of magnetic moment means, up spins electrons of atoms have commanding role than down spins electrons in the systems. The magnetic properties developed in $1C_{atom\text{-}vacancy} - w_{ad} - G$ and $2C_{atoms\text{-}vacancy} - w_{ad} - G$ materials are due to the distribution of unpaired electrons spins in 2s & 2p orbitals of carbon atoms in structures.

4. Conclusions

The physical properties of $w_{ad} - G$, $1C_{atom\text{-}vacancy} - w_{ad} - G$ and $2C_{atoms\text{-}vacancy} - w_{ad} - G$ materials are investigated through first-principles plane wave calculations within the Density Functional Theory. Computational of this work has been done by using Quantum ESPRESSO package. At first, we have prepared stable water adsorbed graphene super cell structure, and then constructed C sites vacancy defects in it. We found that binding energy of defects structures are less than non-defects structure. The value of binding energy decreases

with increase in defects concentrations in graphene material. From the band structure calculations, we found the Dirac cone is formed at the Fermi energy level in $w_{ad}-G$ material; hence it is called zero band gap semiconductor. But, electrons band states are crossing and split, and they are raised slightly above the Fermi energy level in $1C_{atom\text{-}vacancy}-w_{ad}-G$ and $2C_{atoms\text{-}vacancy}-w_{ad}-G$ materials. Hence, C sites vacancy defects in $w_{ad}-G$ material have metallic properties. We have analyzed the DOS and PDOS calculations, and found that $w_{ad}-G$ is non-magnetic material. The non- magnetic $w_{ad}-G$ material changes to magnetic $1C_{atom\text{-}vacancy}-w_{ad}-G$ and $2C_{atoms\text{-}vacancy}-w_{ad}-G$ materials due to the presence of C sites vacancy defects in $w_{ad}-G$ structure. The total magnetic moment of $1C_{atom\text{-}vacancy}-w_{ad}-G$ and $2C_{atoms\text{-}vacancy}-w_{ad}-G$ materials have values $-0.11\ \mu_B$/cell and $0.03\ \mu_B$/cell respectively. The high value of magnetic moment is given by up and down spins states of electrons in 3p orbital of C atoms in vacancy defects structures.

5. Acknowledgements

HKN acknowledges the UGC Nepal Award no. PhD-75/76-S&T-09. NPA acknowledges network project NT-14 of ICTP/OEA and UGC Nepal Grants CRG 073/74 -S & T-01.

References

[1] Geim A, Novoselov K. The rise of graphene. naturematerials, 6: 183–191. March. 2007;.

[2] Xu M, Liang T, Shi M, Chen H. Graphene-like two-dimensional materials. Chemical reviews. 2013;113(5):3766–3798.

[3] Mayorov AS, Gorbachev RV, Morozov SV, Britnell L, Jalil R, Ponomarenko LA, et al. Micrometer-scale ballistic transport in encapsulated graphene at room temperature. Nano letters. 2011;11(6):2396–2399.

[4] Morozov S, Novoselov K, Katsnelson M, Schedin F, Elias D, Jaszczak JA, et al. Giant intrinsic carrier mobilities in graphene and its bilayer. Physical review letters. 2008;100(1):016602.

[5] Novoselov KS, Geim AK, Morozov SV, Jiang D, Katsnelson MI, Grigorieva I, et al. Two-dimensional gas of massless Dirac fermions in graphene. nature. 2005;438(7065):197–200.

[6] Lei JC, Zhang X, Zhou Z. Recent advances in MXene: Preparation, properties, and applications. Frontiers of Physics. 2015;10(3):276–286.

[7] Dávila M, Xian L, Cahangirov S, Rubio A, Le Lay G. Germanene: a novel two-dimensional germanium allotrope akin to graphene and silicene. New Journal of Physics. 2014;16(9):095002.

[8] Balendhran S, Walia S, Nili H, Sriram S, Bhaskaran M. Elemental analogues of graphene: silicene, germanene, stanene, and phosphorene. small. 2015;11(6):640–652.

[9] Lehtinen PO, Foster AS, Ma Y, Krasheninnikov A, Nieminen RM. Irradiation-induced magnetism in graphite: a density functional study. Physical review letters. 2004;93(18):187202.

[10] Yazyev OV, Louie SG. Topological defects in graphene: Dislocations and grain boundaries. Physical Review B. 2010;81(19):195420.

[11] Hashimoto A, Suenaga K, Gloter A, Urita K, Iijima S. Direct evidence for atomic defects in graphene layers. nature. 2004;430(7002):870–873.

[12] Krasheninnikov A, Banhart F. Engineering of nanostructured carbon materials with electron or ion beams. Nature materials. 2007;6(10):723–733.

[13] Crespi VH, Benedict LX, Cohen ML, Louie SG. Prediction of a pure-carbon planar covalent metal. Physical Review B. 1996;53(20):R13303.

[14] Kim Y, Ihm J, Yoon E, Lee GD. Dynamics and stability of divacancy defects in graphene. Physical Review B. 2011;84(7):075445.

[15] Singh R, Kroll P. Magnetism in graphene due to single-atom defects: dependence on the concentration and packing geometry of defects. Journal of Physics: Condensed Matter. 2009;21(19):196002.

[16] Faccio R, Fernández-Werner L, Pardo H, Goyenola C, Ventura ON, Mombrú ÁW. Electronic and structural distortions in graphene induced by carbon vacancies and boron doping. The Journal of Physical Chemistry C. 2010;114(44):18961–18971.

[17] Topsakal M, Aktürk E, Sevinçli H, Ciraci S. First-principles approach to monitoring the band gap and magnetic state of a graphene nanoribbon via its vacancies. Physical Review B. 2008;78(23):235435.

[18] Balog R, Jørgensen B, Nilsson L, Andersen M, Rienks E, Bianchi M, et al. Bandgap opening in graphene induced by patterned hydrogen adsorption. Nature materials. 2010;9(4):315–319.

[19] Robertson AW, Montanari B, He K, Allen CS, Wu YA, Harrison NM, et al. Structural reconstruction of the graphene monovacancy. ACS nano. 2013;7(5):4495–4502.

[20] Yazyev OV, Helm L. Defect-induced magnetism in graphene. Physical Review B. 2007;75(12):125408.

[21] Neupane HK, Adhikari NP. Tuning Structural, Electronic, and Magnetic Properties of C Sites Vacancy Defects in Graphene/MoS2 van der Waals Heterostructure Materials: A First-Principles Study. Advances in Condensed Matter Physics. 2020;2020.

[22] Fedorov A, Popov Z, Fedorov D, Eliseeva N, Serjantova M, Kuzubov A. DFT investigation of the influence of ordered vacancies on elastic and magnetic properties of graphene and graphene-like SiC and BN structures. physica status solidi (b). 2012;249(12):2549–2552.

[23] Hohenberg P, Kohn W. Inhomogeneous electron gas. Physical review. 1964;136(3B):B864.

[24] Giannozzi P, Baroni S, Bonini N, Calandra M, Car R, Cavazzoni C, et al. QUANTUM ESPRESSO: a modular and open-source software project for quantum simulations of materials. Journal of physics: Condensed matter. 2009;21(39):395502.

[25] Perdew JP, Burke K, Ernzerhof M. Generalized gradient approximation made simple. Physical review letters. 1996;77(18):3865.

[26] Martin RM. Electronic structure: basic theory and practical methods. Cambridge university press; 2004.

[27] Pfrommer BG, Côté M, Louie SG, Cohen ML. Relaxation of crystals with the quasi-Newton method. Journal of Computational Physics. 1997;131(1):233–240.

[28] Marzari N, Vanderbilt D, De Vita A, Payne M. Thermal contraction and disordering of the Al (110) surface. Physical review letters. 1999;82(16):3296.

[29] Neupane H, Adhikari N. Structure, electronic and magnetic properties of 2D Graphene-Molybdenum diSulphide (G-MoS2) heterostructure (HS) with vacancy defects at Mo sites. Computational Condensed Matter. 2020;24:e00489.

[30] Hou Z, Wang X, Ikeda T, Terakura K, Oshima M, Kakimoto Ma, et al. Interplay between nitrogen dopants and native point defects in graphene. Physical Review B. 2012;85(16):165439.